Journal of
Materials Chemistry A

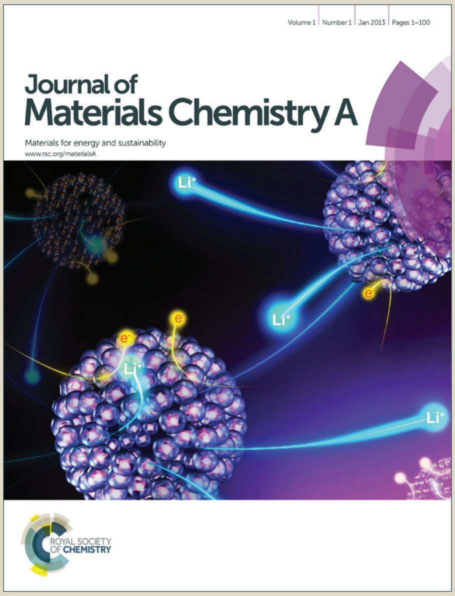

ROYAL SOCIETY
OF CHEMISTRY

www.rsc.org/materialsA

Journal of Materials Chemistry A

Dynamic Article Links ►

Cite this: DOI: 10.1039/c0xx00000x

www.rsc.org/xxxxxx

Paper

Preparation of Highly Photoluminescent Sulfur-doped Carbon Dots for Fe(III) Detection

Quan Xu*,[a] Peng Pu,[a] Jungang Zhao,[a] Chenbo Dong,[b] Chun Gao,[c] Yusheng Chen,[c] Jiarui Chen,[d] Yao Liu[a] and Hongjun Zhou[a]

Received (in XXX, XXX) Xth XXXXXXXXX 20XX, Accepted Xth XXXXXXXXX 20XX

DOI: 10.1039/b000000xu

Carbon dots (C-dots) with sulfur-doped (S-doped) was synthesized using a simple and straightforward hydrothermal method. The as-prepared S-doped C-dots exhibit significant high fluorescence quantum yield (67%) and unique emission property. The form spherical shaped S-doped C-dots have average diameter 4.6 nm and the fluorescence of S-doped C-dots can be effectively and selectively quenched by Fe^{3+} ions. Thus, S-doped C-dots were applied as probes toward Fe^{3+} detection exhibiting a limit as well as 0.1 μM

Introduction

Carbon nanomaterials have attracted an extensive attention by researchers due to its optical, electronic and biocompatible properties.[1-9] Most of the carbon nanomaterials have unique fluorescent property, including carbon nanotubes and graphene. Among these carbon based nanomaterials, Carbon nanodots (C-dots) are one of most promising fluorescent nanoparticles. Due to its low low-toxicity and easy-fabrication, C-dots have been widely used in the different fields, such as biosensors,[3, 10-12] bioimaging,[13, 14] optoelectronic,[15] photocatalysis,[16] etc.

In recent years, heteroatom doping was reported to improve the optic and electronic property of carbon nanomaterials[17, 18]. Especially, heteroatom doped C-dots exhibited a significant improvement in its electronic and fluorescence property, which attract extensive interest.[3, 4, 11, 19-25] For example, Yang et al. reported a hydrothermal method to synthesize nitrogen-doped C-dots with citric acid and ethylenediamine as precursors. The quantum yield of the doped C-dots can reach up to 80%, which is almost equal to that of fluorescent dyes.[21] By using similar hydrothermal method, nitrogen and sulfur co-doped C-dots were prepared by Yu *et al* using citric acid and L-cysteine as precursor, which also exhibited quantum yield (QY) up to 73%. [22]However, those high quantum yield C-dots are prepared with nitrogen doping or nitrogen/sulfur co-doping. So far, to our best knowledge, sulfur-doped C-dots have never been reported to reach high photoluminescence (QY> 50%). In this study, S-doped C-dots with significantly QY (up to 67%) were first time prepared via hydrothermal method, simply by using sodium citrate and sodium thiosulfate as precursors. The chemical/physical properties of this novel S-doped C-dots were studied using series characterization technologies including transmission electron microscopy (TEM), fluorescence spectroscopy, X-ray photoelectron spectroscopy (XPS) and fourier transform infrared spectroscopy (FTIR). Furthermore, the as-prepared S-doped C-dots are applied as nanosensor probes for Fe^{3+} detection.

Experimental

Materials

Sodium citrate and sodium thiosulfate were purchased from Tianjin Guangfu technology development Co., Ltd. Ferric trichloride was obtained from Sinopharm Chemical Reagent Co., Ltd. The reagents used in experiments were analytical grade and were used without further purification. All solutions were prepared using deionized water from Dongguanshi Qianjing environmental equipment Co., Ltd

Synthesis of S-doped C-dots

S-doped C-dots were synthesized using hydrothermal method. Briefly, 25 mL sodium citrate solution (0.1 M) and sodium thiosulfate were added into a 50 mL teflon-lined stainless steel autoclave. After that, the autoclave was kept at different temperature for 6 h. The product can be used after filtered with cylinder filtration membrane filter (0.22 μm).

Characterization

Transmission electron microscopy (TEM) (Model JEM-2100 and JEM-2100F, JEOL) was used to characterize the surface morphology of the as-prepared C-dots. The UV-vis absorption spectra of products were recorded by Jasco V-570 UV-vis spectrometer. The fluorescence measurements were performed with a Cary Eclipse fluorescence spectrophotometer (Varian, Inc.). Specially, samples were placed in a 10 mm optical path length quartz fluorescence cuvette. The sample was excited at 350 nm, and the range of emission spectra were 400–530 nm. The emission slit and the exciting slit were both 2.5 nm. X-ray photoelectron spectroscopy (XPS) analysis of sample was recorded using ESCALAB 250 spectrometer with a mono X-Ray source Al Kα excitation (1486.6 eV). Binding energy calibration was based on C_{1s} at 284.6 eV. X-ray Photoelectron Spectroscopy (XPS) was recorded using ESCALAB 250 spectrometer with a mono X-Ray source Al Kα excitation (1486.6 eV). Binding energy calibration was based on C_{1s} at 284.6 eV.

Determination of fluorescence quantum yield

Quantum yield (QY) measurement was performed according to the previously established procedure. Quinine sulfate dispersed in 0.1M H_2SO_4 (QY 54%) was used as a standard as reported in papers.[20, 26] The absorbance of the solution for S-doped C-dots and quinine sulfate were kept below 0.05 at 350 nm.

Detection of the concentration of Fe^{3+}

General, 5 μL C-dots was diluted into 1 mL with deionized water and the fluorescence intensity in 440nm excited by light of 350 nm was measured, which is defined as the fluorescence intensity of the starting point (F_0). After the Fe^{3+} solution was added to the mixture obtained, the fluorescence intensity was measured after 1 minute. The exciting slit and the emission slit were 2.5 nm and 5 nm, separately.

Results and discussion

Optimization of synthesis conditions

In this study, sodium citrate, a kind of sodium salt, was firstly selected as the carbon source for preparing carbon dots, while sodium thiosulfate was adopted as the source of sulfur. (Figure 1(a)) The fluorescent property of the S-doped C-dots is affected by several factors, such as the ratio between sulphur source and carbon source, the temperature of hydrothermal method and time of reaction. Thus, the experimental condition needs to be optimized in order to achieve S-doped C-dots with high fluorescent properties. As the carbon source, the concentration of sodium citrate was fixed to be 0.1 M. The ratio of carbon source and sulfur source was varied via alternation of the concentration of sodium thiosulfate. It was found that the optimum ratio of sulfur source and carbon source was 3 (Figure 1(b)). When the ratio of sulfur source and carbon source was decreased below or increased above 3, there was significant decrease for the QY of S-doped C-dots. As the ratio of sulphur source and carbon source increase, more sulphur would be doped into the carbon dot, which can increase the QY. Although the mechanism is not clear, there is a possibility that too much sulphur would block the passivated surface defect, which lead to the decrease of QY. The temperature of hydrothermal method was also optimized. The temperature investigated in this study were 160, 180, 200, 220, and 240 °C, respectively, while the ratio of carbon source and sulfur source was 1:3 and the time for hydrothermal process was 6 h(Figure 1(c)). The result clearly demonstrated that QY increased gradually up to a maximum value with the increasing of temperature to 200 °C, followed by an decrease for further increasing the temperature. According to Figure 1(d), it can be observed the QY increased with the increase of reaction time before 6h. When the reaction time is prolonged to 8h, there was no apparent change of QY. In summary, the optimum experimental conditions are as follows: 0.1M sodium citrate, 0.3M sodium thiosulfate, 200 °C and 6 h.

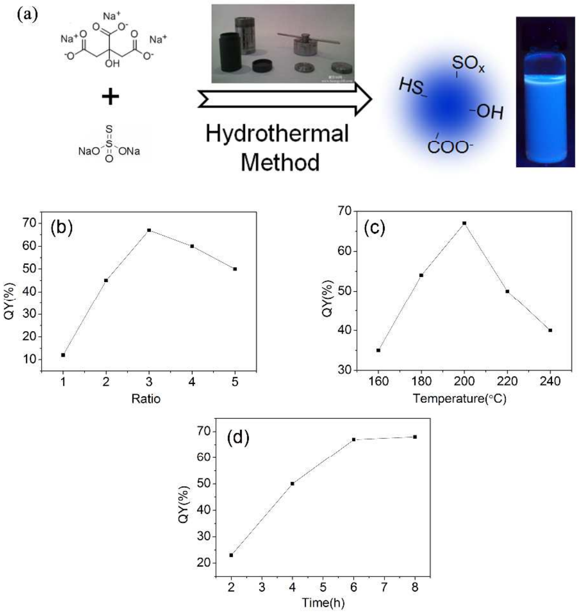

Figure 1. (a) graphical of the synthesis of S-doped C-dots with blue luminescence; quantum yield (QY) of S-doped C-dots as a function of (b) ratio of sulfur source and carbon source; (c) the temperature of hydrothermal method ; (d) time of reaction.

Characterization

The S-doped C-dots prepared under optimum experimental conditions were characterized by TEM, AFM and fluorescence spectroscopy. The TEM image (Figure 2(a)) and HRTEM image (Figure 2(b)) demonstrated that the S-doped C-dots have spherical shape and were well separated in solution, which was confirmed by AFM results (Figure S1). S-doped C-dots also exhibited a narrow size distribution with an average size of around 4.6 nm (Figure 2(c)). Figure 2(d) shows the excitation spectrum and several emission spectra excited using light with different wavelengths. It is illustrated that the as-prepared S-doped C-dots exhibited great emission with λ_{em} at 440 nm, such emission is independent of λ_{ex} for λ_{ex} changed from 300 nm to 400 nm. It could attribute to the homogeneous surface structures and size of S-doped C-dots.[27] In our research, it is observed that the photoluminescence lifetime of the as-prepared S-doped C-dots is 11.26 ns (Figure S3).

The fluorescence quantum yield for the as-prepared S-doped C-dots is determined by calibrating against quinine sulfate in 0.1 M H_2SO_4 solution (Figure 2(e)). The fluorescence quantum yield of quinine sulfate in 0.1 M H_2SO_4 solution is 54% and the fluorescence quantum yield of C-dots is 67% which is the highest quantum yield generated by S-doped C-dots, which never been reported in previous studies. Although the photoluminescence mechanism of C-dots is not clear, several hypotheses have been proposed according to pervious researches, such as energy traps and electronic conjugated structure. [28, 29] For heteroatom doped C-dots, it has been reported that the surface detect passivated by heteroatom would act as excitation energy traps and impact on the photoluminescence of C-dots.[30] Especially, the sulfur atom in C-dots plays a role as catalyst for oxidation reduction reaction,[31] which introduce more passivated surface detect of C-dots and further enhance photoluminescence. Due to this property, doping sulfur is used to increase the photoluminescence of C-dots in recent researches.[22]

The influence of pH on the fluorescent intensity of the S-doped C-dots was also evaluated. Figure 2(f) shows the fluorescent intensity in 440 nm excited by 350 nm, while the pH of solution changed. It is demonstrated that the fluorescent intensity of S-doped C-dots is strong and stable in a wide range of pH values (i.e. pH range from 6 to 10). However, as the pH value decrease to 5 or higher than 10, the intensity decreased sharply and irreversibly. The wide range of effective fluorescence makes S-doped C-dots a promising material candidate for biological application.

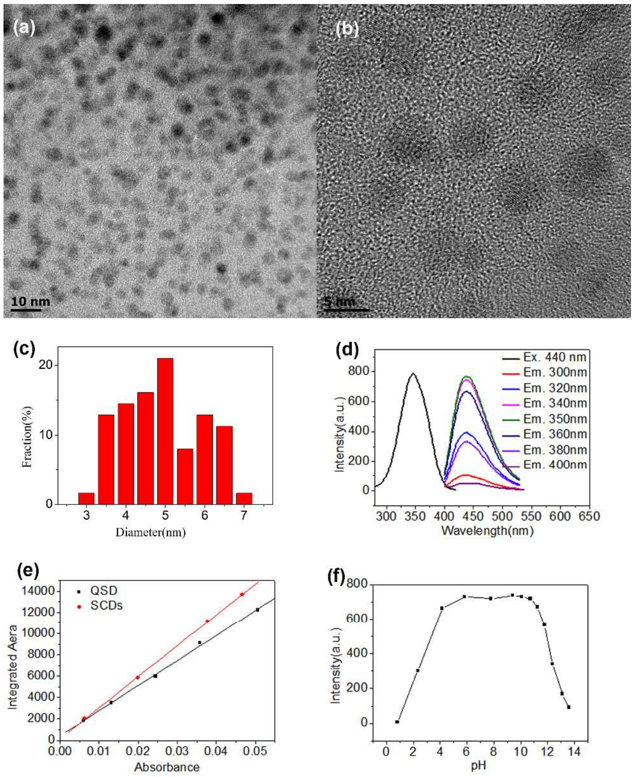

Figure 2 (a) TEM image of S-doped C-dots; (b) HRTEM image of S-doped C-dots; (c) the diameter distribution of S-doped C-dots; (d) photoluminescence spectrum of the S-doped C-dots; (e) the determination of fluorescence quantum yield for the S-doped C-dots; (f) the fluorescent intensity in 440 nm excited by 350 nm as a function of pH.

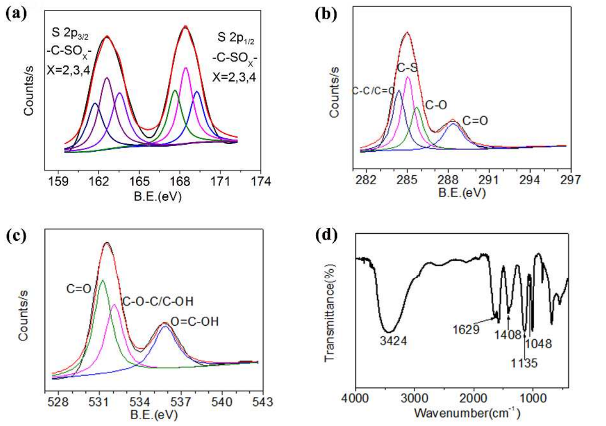

Figure 3(a) – (c) High-resolution S_{2p}, C_{1s}, O_{1s} XPS spectra for S-doped C-dots; (d) FTIR of S-doped C-dots.

The chemical structure of S-doped C-dots was further characterized by X-ray photoelectron spectroscopy (XPS) and fourier transform infrared spectroscopy (FTIR). Binding energy calibration was based on C1s at 285.0 eV. The high-resolution S_{2p}, C_{1s} and O_{1s} of S-doped C-dots are demonstrated in Figure 3(a)-(c), separately. According to Figure 3(a), the S_{2p} spectrum consists of two peaks, which centred at 162.7 eV (S $_{2P3/2}$) and 168.3 ev (S $_{2P1/2}$).The two peaks could be deconvoluted three peaks, attributed to –C-SO$_x$ (x=2, 3, 4).[32-34] The C_{1s} spectrum can be resolved as follows: C-C and C=C at 285.0 eV, C-S at 285.6 eV, C-O at 286.3 eV, and C=O at 289.0 eV (Figure 3(b)).[20, 35-39] As shown in Figure 3(c), the O_{1s} spectrum have three peaks centring at 531.3 eV, 532.1 eV and 535.9 eV, which could be attributed to C=O, C-O-C/C-OH, and. O=C-OH[3, 40, 41] FTIR spectrum of the S-doped C-dots (Figure 3(d)) demonstrates the presence of the same groups with XPS results. The peak at 1048 cm^{-1} is attributed to –SO^{3-}, C–O, and C–O–C bonds.[20] The peak at 1135 cm^{-1} is ascribed to the C–O, and C–S bonds. The peak at 1408 cm^{-1} can be ascribed to the COO^{-} group when the peak at 1629 cm^{-1} is ascribed to the C=O stretching vibration. In addition, the broad band at 3424 cm^{-1} appears because of O-H bond. [42, 43]

Detection of the concentration of Fe^{3+}

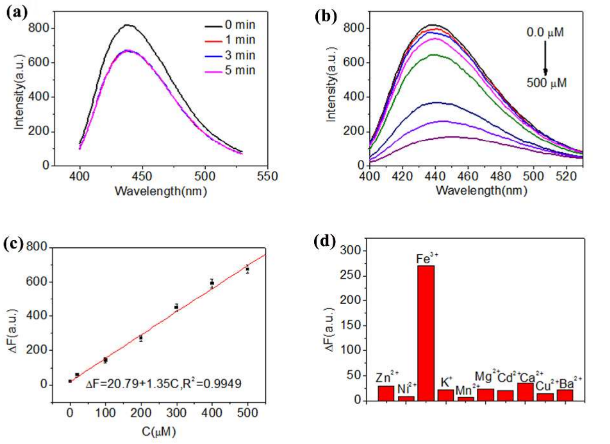

Figure 4(a) time-dependent fluorescence changes of C-dots in the presence of Fe^{3+} (100 μM); (b) emission spectra of the C-dots solution with different concentration of Fe^{3+} (0, 1, 20, 100, 200, 300, 400, and 500 μM); (c) the change of fluorescence intensity of S-doped C-dots solution versus the concentration of Fe^{3+}; Error bars in Figure 4(c) represent the standard deviations of three independent measurements. (d) the change of fluorescent intensity in 440nm for S-doped C-dots in the presence of various metal ions.

We successfully synthesized S-doped C-dots with excellent properties using hydrothermal method involving sodium citrate solution and sodium thiosulfate as precursor. It is found that the as-prepared S-doped C-dots are sensitive toward Fe^{3+}, which is indispensable for metabolic processes of all living systems.[44] The photoluminescence quenching by Fe^{3+} is believed to be related to the fast electron transfer process between Fe^{3+} and carbon dots. Fe^{3+} was known to be able to absorb on the surface of carbon dots and coordinate with phenolic hydroxyl group on edge of carbon dot.[45] Due to this coordination interaction, electron in the excited state of S-doped C-dots would transfer to the unfilled orbit of Fe^{3+} and lead to nonradiative electron/hole recombination, which results in the fluorescence quenching. This hypothesis was proved by previous researches, in which Fe^{3+} was found to significantly shorten the fluorescence lifetime of S-doped C-dots.[46] On the other hand, due to the low electronegativity of heteratom sulfur on the edge of S-doped C-dots, the surface electron density of oxygen atoms around sulfur would trend to form coordination interaction with Fe^{3+}, which further facilitates photoluminescence quenching.[46]

The fluorescence intensity decreases apparently, when Fe^{3+} is added into the solution containing S-doped C-dots. Figure 4(a) showed the time-dependent fluorescence quenching of the S-doped C-dots in the presence of Fe^{3+} (100 μM). The results indicated that the fluorescence intensity changed inconspicuously after 1 min, thus 1 min was chose as the detection time in the following experiment. We use ΔF as a signal for the detection of Fe^{3+}, where $\Delta F = F_0 - F_1$. F_0 is the fluorescence intensity of the starting point, before the Fe^{3+} was introduced into the solution containing S-doped C-dots. After the Fe^{3+} was added into the mixture, the fluorescence intensity was measured after 1 minute (F1). Figure 3(b) showed the degree of quenching effect of the fluorescence of C-dots with different concentration of Fe^{3+} for a fixed time interval of 1 min. It can be seen that the fluorescence intensity decreases apparent with the increase of the concentration of Fe^{3+}. Hence, S-doped C-dots could be used as probes for the fluorescence turn-off detection of Fe^{3+}. The resulting calibration curve for Fe^{3+} displayed good linearity for concentrations ranging from 1 to 500 μM with a correlation coefficient of 0.9949 (Figure 3(c)). The detection limit was as low as 0.1 μM based on three times the standard deviation rule, which could compare favorably with those of previous reports for Fe^{3+} detection[21, 38, 47]. The selectivity of the proposed Fe^{3+} sensor is evaluated by a control experiment. Firstly, 200 μM of various metal ions, including Zn^{2+}, Ni^{2+}, Fe^{3+}, K^+, Mn^{2+}, Mg^{2+},Cd^{2+}, Ca^{2+},Cu^{2+}, Ba^{2+} were added into the S-doped C-dots solution, and the change of fluorescent intensity in 440 nm were then recorded. As demonstrated in Figure 4(d), significant fluorescent quenching effect was observed with the addition of 200 μM Fe^{3+}, while the influence of other metal ions is almost negligible. The anti-interference ability study is one of the most important evaluations for the biosensor. Figure S4 shows the ΔF of 200μM Fe^{3+} (see "Fe^{3+}" in Figure S4). Then the additions of 200μM Zn^{2+} (see "Zn^{2+}" in Figure S4), Ni^{2+} (see "Ni^{2+}" in Figure S4), K^+ (see "K^+" in Figure S4), Mn^{2+} (see "Mn^{2+}" in Figure S4), Mg^{2+} (see "Mg^{2+}" in Figure S4),Cd^{2+} (see "Cd^{2+}" in Figure S4), Ca^{2+} (see "Ca^{2+}" in Figure S4),Cu^{2+} (see "Cu^{2+}" in Figure S4), Ba^{2+} (see "Ba^{2+}" in Figure S4) did not cause observable changes of the ΔF of 200μM Fe^{3+}. It was proved that the biosensor can provide credible anti-interference ability.

Conclusions

S-doped C-dots with high fluorescence quantum yield (67%) were firstly synthesized using hydrothermal method adopting sodium citrate and sodium thiosulfate as precursor. It is found the spherical shaped S-doped C-dots have an average size of 4.6 nm as well as great dispersity in solution. The excellent fluorescent properties of S-doped C-dots make them a promising material candidate used in biological field. Furthermore, the as-prepared S-doped C-dots could be used as probes without any modification for the fluorescence turn-off detection of Fe^{3+} in the range of 1 – 500 μM with the limit of detection is 0.1 μM.

Acknowledgments

We thank Science Foundation of China University of Petroleum Beijing (No. 2462014YJRC011) and Beijing Key Laboratory of Biogas High Value Utilization for the support.

Notes and references

[a] *Institute of New Energy, State Key Laboratory of Heavy Oil Processing, China University of Petroleum (Beijing), Beijing, 102249, China*
[b] *Department of Civil and Environmental Engineering, Rice University, Houston, Texas 77005, USA*
[c] *Department of Chemical Engineering, University of Akron, 44306, USA*
[d] *Department of Chemical Engineering, Xi'an Jiaotong University, Xi'an, Shaanxi 710049, China*

Email: xuquan@cup.edu.cn

1 S. Barman and M. Sadhukhan, *J. Mater. Chem.*, 2012, **22**, 21832.
2 Y. Song, W. Shi, W. Chen, X. Li and H. Ma, *J. Mater. Chem.*, 2012, **22**, 12568.
3 S. Yang, J. Sun, X. Li, W. Zhou, Z. Wang, P. He, G. Ding, X. Xie, Z. Kang and M. Jiang, *J .Mater. Chem. A*, 2014, **2**, 8660.
4 S. Chandra, P. Patra, S. H. Pathan, S. Roy, S. Mitra, A. Layek, R. Bhar, P. Pramanik and A. Goswami, *J. Mater. Chem. B*, 2013, **1**, 2375.
5 P. G. Luo, S. Sahu, S.-T. Yang, S. K. Sonkar, J. Wang, H. Wang, G. E. LeCroy, L. Cao and Y.-P. Sun, *J. Mater. Chem. B*, 2013, **1**, 2116.
6 N. Na, T. Liu, S. Xu, Y. Zhang, D. He, L. Huang and J. Ouyang, *J. Mater. Chem. B*, 2013, **1**, 787.
7 Z. L. Wu, P. Zhang, M. X. Gao, C. F. Liu, W. Wang, F. Leng and C. Z. Huang, *J. Mater. Chem. B*, **1**, 2868.
8 Y. Liu, C. Y. Liu and Z. Y.. Zhang, *J. Mater. Chem. C*, 2013, **1**, 4902.
9 L. Zhu, Y. Yin, C.-F. Wang and S. Chen, *J. Mater. Chem. C*, 2013, **1**, 4925.
10 X. Qin, W. Lu, A. M. Asiri, A. O. Al-Youbi and X. Sun, *Sensor. Actuat. B-Chem.*, 2013, **184**, 156.
11 R. Zhang and W. Chen, *Biosens. Bioelectron.*, 2014, **55**, 83.
12 X. Yang, Y. Luo, S. Zhu, Y. Feng, Y. Zhuo and Y. Dou, *Biosens. Bioelectron.*, 2014, **56**, 6.

13 Q. Li, T. Y. Ohulchanskyy, R. Liu, K. Koynov, D. Wu, A. Best, R. Kumar, A. Bonoiu and P. N. Prasad, *J. Phy. Chem. C*, 2010, **114**, 12062.

14 X. Zhang, S. Wang, C. Zhu, M. Liu, Y. Ji, L. Feng, L. Tao and Y. Wei, *J. Colloid. Interf. Sci.*, 2013, **397**, 39.

15 V. Gupta, N. Chaudhary, R. Srivastava, G. D. Sharma, R. Bhardwaj and S. Chand, *J. Am. Chem. Soc.*, 2011, **133**, 9960.

16 Y. Han, H. Huang, H. Zhang, Y. Liu, X. Han, R. Liu, H. Li and Z. Kang, *ACS. Catal.*, 2014, **4**, 781.

17 R. Ye, C. Xiang, J. Lin, Z. Peng, K. Huang, Z. Yan, N. P. Cook, E. L. Samuel, C. C. Hwang, G. Ruan, G. Ceriotti, A. R. Raji, A. A. Marti and J. M. Tour, *Nat. Commun.*, 2013, **4**, 2943.

18 M. Li, L. Zhang, Q. Xu, J. Niu and Z. Xia, *J. Catal.,* 2014, **314**, 66.

19 Y. Xu, M. Wu, Y. Liu, X. Z. Feng, X. B. Yin, X. W. He and Y. K. Zhang, *Chem.-Eur. J.*, 2013, **19**, 2276.

20 D. Sun, R. Ban, P.-H. Zhang, G.-H. Wu, J.-R. Zhang and J.J. Zhu, *Carbon*, 2013, **64**, 424.

21 S. Zhu, Q. Meng, L. Wang, J. Zhang, Y. Song, H. Jin, K. Zhang, H. Sun, H. Wang and B. Yang, *Angew. Chem. Int. Ed. Engl.*, 2013, **52**, 3953.

22 Y. Dong, H. Pang, H. B. Yang, C. Guo, J. Shao, Y. Chi, C. M. Li and T. Yu, *Angew. Chem. Int. Ed. Engl.*, 2013, **52**, 7800.

23 Z. Qian, X. Shan, L. Chai, J. Ma, J. Chen and H. Feng, *Acs. Appl. Mater. Inter.*, 2014, **6**, 6797.

24 M. Xu, G. He, Z. Li, F. He, F. Gao, Y. Su, L. Zhang, Z. Yang and Y. Zhang, *Nanoscale*, 2014, **6**, 10307

25 Z. Yang, M. Xu, Y. Liu, F. He, F. Gao, Y. Su, H. Wei and Y. Zhang, *Nanoscale*, 2014, **6**, 1890

26 Q. Liang, W. Ma, Y. Shi, Z. Li and X. Yang, *Carbon*, 2013, **60**, 421

27 Z. Huang, F. Lin, M. Hu, C. Li, T. Xu, C. Chen and X. Guo, *J. Lumin.*, 2014, **151**, 100

28 Y.-P. Sun, B. Zhou, Y. Lin, W. Wang, K. A. S. Fernando, P. Pathak, M. J. Meziani, B. A. Harruff, X. Wang, H. Wang, P. G. Luo, H. Yang, M. E. Kose, B. Chen, L. M. Veca and S.-Y. Xie, *J. Am. Chem. Soc.,* 2006, 128, 7756

29 X. Wang, L. Cao, S.-T. Yang, F. Lu, M. J. Meziani, L. Tian, K. W. Sun, M. A. Bloodgood and Y.-P. Sun, *Angew. Chem., Int. Ed.,* 2010, **49**, 5310

30 Y.-P. Sun, X. Wang, F. Lu, L. Cao, M. J. Meziani, P. G. Luo, L. Gu and L. M. Veca, *J. Phys. Chem. C*, 2008, **112**, 18295

31 J. Liang, Y. Jiao, M. Jaroniec and S. Z. Qiao, *Angew. Chem., Int. Ed.,* 2012, **51**, 11496

32 S. Yang, L. Zhi, K. Tang, X. Feng, J. Maier and K. Müllen, *Adv. Funct. Mater.*, 2012, **22**, 3634.

33 Y. Li, J. Wang, X. Li, D. Geng, M. N. Banis, Y. Tang, D. Wang, R. Li, T. K. Sham and X. Sun, *J. Mater. Chem.*, 2012, **22**, 20170.

34 Z. Yang, Z. Yao, G. Li, G. Fang, H. Nie, Z. Liu, X. Zhou, X. a. Chen and S. Huang, *ACS Nano*, 2011, **6**, 205.

35 J. P. Paraknowitsch, Y. Zhang, B. Wienert and A. Thomas, *Chem. Commun.*, 2013, **49**, 1208.

36 R.J. Fan, Q. Sun, L. Zhang, Y. Zhang and A.-H. Lu, *Carbon*, 2014, **71**, 87.

37 D. Tan, Y. Yamada, S. Zhou, Y. Shimotsuma, K. Miura and J. Qiu, *Carbon*, 2014, **69**, 638.

38 Y. Liu, N. Xiao, N. Gong, H. Wang, X. Shi, W. Gu and L. Ye, *Carbon*, 2014, **68**, 258.

39 A. B. Bourlinos, M. A. Karakassides, A. Kouloumpis, D. Gournis, A. Bakandritsos, I. Papagiannouli, P. Aloukos, S. Couris, K. Hola, R. Zboril, M. Krysmann and E. P. Giannelis, *Carbon*, 2013, **61**, 640.

40 H. Nie, M. Li, Q. Li, S. Liang, Y. Tan, L. Sheng, W. Shi and S. X.-A. Zhang, *Chem. Mater.*, 2014, **26**, 3104.

41 K. S. Prasad, R. Pallela, D.-M. Kim and Y.-B. Shim, *Part. Part. Syst. Char.*, 2013, **30**, 557.

42 H. Peng and J. Travas-Sejdic, *Chem. Mater.*, 2009, **21**, 5563.

43 S. Zhu, J. Zhang, S. Tang, C. Qiao, L. Wang, H. Wang, X. Liu, B. Li, Y. Li, W. Yu, X. Wang, H. Sun and B. Yang, *Adv. Funct. Mater.*, 2012, **22**, 4732.

44 A. Zhao, C. Zhao, M. Li, J. Ren and X. Qu, *Anal. Chim. Acta.*, 2014, **809**, 128.

45 K. Qu, J. Wang, J. Ren and X. Qu, *Chemistry*, 2013, **19**, 7243

46 S. Li, Y. Li, J. Cao, J. Zhu, L. Fan and X. Li, *Anal. Chem.*, 2014, **86**, 10201

47 J. Ju and W. Chen, *Biosens. Bioelectron.*, 2014, **58**, 219

Graphic of abstract

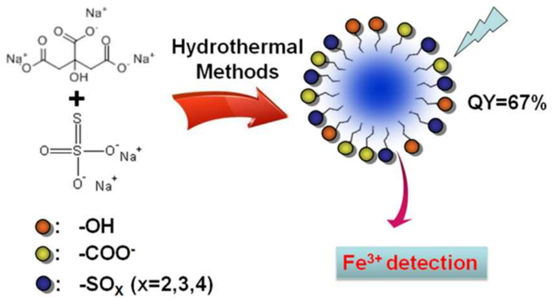

Sulfur-doped carbon dots was synthesized by one-step hydrothermal method and exhibited high fluorescence quantum yield (67%) and exceptional emission property.